Naval Research Laboratory

Washington, DC 20375-5320

NRL/MR/6790--08-9156

Optical Quality of High-Power Laser Beams in Lenses

JOSEPH PEÑANO
PHILLIP SPRANGLE
ANTONIO TING
RICHARD FISCHER

Beam Physics Branch
Plasma Physics Division

BAHMAN HAFIZI

Icarus Research Inc.
Bethesda, Maryland

PHILIP SERAFIM

Northeastern University
Boston, Massachusetts

October 31, 2008

REPORT DOCUMENTATION PAGE

Form Approved
OMB No. 0704-0188

1. REPORT DATE *(DD-MM-YYYY)*	2. REPORT TYPE	3. DATES COVERED *(From - To)*
31-10-2008	Interim	March 2008 – September 2008

4. TITLE AND SUBTITLE

Optical Quality of High-Power Laser Beams in Lenses

5a. CONTRACT NUMBER

5b. GRANT NUMBER

5c. PROGRAM ELEMENT NUMBER
67-9252-08

6. AUTHOR(S)

Joseph Peñano, Phillip Sprangle, Antonio Ting, Richard Fischer, Bahman Hafizi,* and Philip Serafim†

5d. PROJECT NUMBER

5e. TASK NUMBER

5f. WORK UNIT NUMBER

7. PERFORMING ORGANIZATION NAME(S) AND ADDRESS(ES)

Naval Research Laboratory
4555 Overlook Avenue, SW
Washington, DC 20375

8. PERFORMING ORGANIZATION REPORT NUMBER

NRL/MR/6790--08-9156

9. SPONSORING / MONITORING AGENCY NAME(S) AND ADDRESS(ES)

Office of Naval Research
875 North Randolph Street
Arlington, VA 22203-1995

10. SPONSOR / MONITOR'S ACRONYM(S)

ONR

11. SPONSOR / MONITOR'S REPORT NUMBER(S)

12. DISTRIBUTION / AVAILABILITY STATEMENT

Approved for public release; distribution is unlimited.

13. SUPPLEMENTARY NOTES

*Icarus Research, Inc., P.O. Box 30780, Bethesda, MD 20814-0780
†Department of Electrical and Computer Engineering, Northeastern University, Boston, MA 02115

14. ABSTRACT

We analyze the propagation of a high-power laser beam through a lens and calculate the optical beam quality resulting from geometrical aberrations and thermal nonlinearities. We present a general ray optics formulation, including diffraction effects, for propagation through a nonlinear medium. An analytical expression for the beam quality parameter M^2 is derived that includes the lowest-order effects of geometrical and thermal aberrations in a thin lens. A ray optics simulation including thermal effects is used to model propagation through a multi-lens optical beam expander of the type used in recent long-range, high-power fiber laser experiments.

15. SUBJECT TERMS

High-power laser beams
Beam quality
Thermal effects
Lenses

16. SECURITY CLASSIFICATION OF:			17. LIMITATION OF ABSTRACT	18. NUMBER OF PAGES	19a. NAME OF RESPONSIBLE PERSON
a. REPORT	b. ABSTRACT	c. THIS PAGE			Joseph Peñano
Unclassified	Unclassified	Unclassified	UL	32	19b. TELEPHONE NUMBER *(include area code)* (202) 767-8367

This page intentionally left blank.

CONTENTS

Abstract 1

I. Introduction 2

II. Ray Optics Formulation 3

i) Ray Equations 3

ii) Ray Distribution 4

iii) Optical Beam Quality 5

iv) Diffraction 6

III. Effects of Nonlinearities on Optical Beam Quality 6

IV. Thermal Nonlinearity in Lenses 8

V. Numerical Simulation 13

i) Single Lens 13

ii) NRL Beam Expander 14

VI. Discussion 16

VII. Conclusions 17

Acknowledgments 18

Optical Quality of High-Power Laser Beams in Lenses

Joseph Peñano,[1*] Phillip Sprangle,[1] Antonio Ting,[1] Richard Fischer,[1]

Bahman Hafizi,[2] and Phillip Serafim[3]

[1]*Naval Research Laboratory, 4555 Overlook Ave. SW, Washington, D.C. 2037*

[2]*Icarus Research Inc., P.O. Box 30780, Bethesda, MD 20824-0780*

[3]*Dept. of Electrical and Computer Engineering, Northeastern University, Boston, MA 02115*

Abstract

We analyze the propagation of a high-power laser beam through a lens and calculate the optical beam quality resulting from geometrical aberrations and thermal nonlinearities. We present a general ray optics formulation, including diffraction effects, for propagation through a nonlinear medium. An analytical expression for the beam quality parameter M^2 is derived that includes the lowest-order effects of geometrical and thermal aberrations in a thin lens. A ray optics simulation including thermal effects is used to model propagation through a multi-lens optical beam expander of the type used in recent long-range, high-power fiber laser experiments.

Manuscript approved October 7, 2008

I. Introduction

High energy laser systems for directed energy applications, e.g., high-power fiber lasers [1], are prone to nonlinearities in the optics that degrade the optical beam quality and result in a large spreading angle. For high-power lasers, the beam degradation due to nonlinearities in transmissive optics may dominate atmospheric effects such as turbulence, among others [2]. The objective of this Paper is to analyze and numerically simulate the effects of geometrical and thermal aberrations in lenses on the optical beam quality of a high-power laser beam.

Recent high-power fiber laser experiments conducted by the Naval Research Laboratory (NRL) at the Naval Surface Warfare Center (NSWC, range 1.2 km) and the Starfire Optical Range (SOR, range 3.2 km) propagated a number of multi-kW fiber laser beams through the atmosphere and incoherently combined the beams onto a 10 cm radius target. In both experiments, each beam passed through a multi-lens beam expander configuration. In the NSWC experiments, 3kW (cw) was propagated with an efficiency > 90% at a range of 1.2 km [3]. It was observed that, as the power of an individual fiber laser was increased to ~1 kW, the laser spot size on target expanded and was deflected, and the propagation efficiency dropped. Analysis and simulations indicate that, at these power levels and propagation geometries, thermal blooming in the atmosphere can be mitigated by using a fan near the laser source to induce air flow across the beam path. However, because of high laser intensity emerging from the fiber, thermal nonlinearities in the transmissive optics cannot be mitigated in this manner and result in the observed beam degradation.

In this Paper, we analyze the propagation physics of a high-power laser beam through an optical beam expander consisting of a system of expanding and focusing lenses. In particular, we analyze the optical beam quality resulting from geometrical aberrations and thermal

nonlinearities. Section II presents the general ray optics formulation for propagation through a nonlinear lens. We discuss how to model diffraction effects using a ray optics approach and define the optical beam quality parameter M^2 [2]. In Section III we discuss potential sources of nonlinearity in a lens and analyze the lowest order effects of spherical and thermal nonlinearities in a thin lens on beam quality. Section IV presents results of ray optics simulations on systems of lenses. We examine thermal effects in a single, optically thick lens and model a multi-lens beam expander similar to that used in recent NRL experiments. In Section V, we discuss our theoretical findings in the context of recent experimental results and present conclusions in Section VI.

II. Ray Optics Formulation

The ray optics equations describing the propagation of a ray through a medium with a non-uniform refractive index $n(\mathbf{r})$ are $d\mathbf{r}/dt = \partial\omega/\partial\mathbf{k}$, and $d\mathbf{k}/dt = -\partial\omega/\partial\mathbf{r}$, where $\mathbf{r}$ is the transverse position of the ray and $k = |\mathbf{k}|$ is the magnitude of the wave vector. The angular radiation frequency $\omega = ck/n(\mathbf{r})$ serves as the Hamiltonian and $d\omega/dt = 0$ [4].

i) Ray Equations

Transforming to the independent variable z, the ray optics equations can be combined to give

$$\frac{\partial^2 \tilde{x}}{\partial z^2} = \frac{1}{\tilde{n}}\left(1 + \left(\frac{\partial \tilde{x}}{\partial z}\right)^2 + \left(\frac{\partial \tilde{y}}{\partial z}\right)^2\right)\left(\frac{\partial \tilde{n}}{\partial \tilde{x}} - \frac{\partial \tilde{x}}{\partial z}\frac{\partial \tilde{n}}{\partial z}\right), \tag{1a}$$

$$\frac{\partial^2 \tilde{y}}{\partial z^2} = \frac{1}{\tilde{n}}\left(1 + \left(\frac{\partial \tilde{x}}{\partial z}\right)^2 + \left(\frac{\partial \tilde{y}}{\partial z}\right)^2\right)\left(\frac{\partial \tilde{n}}{\partial \tilde{y}} - \frac{\partial \tilde{y}}{\partial z}\frac{\partial \tilde{n}}{\partial z}\right), \tag{1b}$$

where $\tilde{x}(z,t)$ and $\tilde{y}(z,t)$ denote the transverse coordinates of the ray and $\tilde{n}(\tilde{x}(z),\tilde{y}(z),z,t)$ is the refractive index evaluated at the position of the ray at time t. Thermal effects cause the refractive index to vary with time. In deriving Eqs. (1), we have made the quasi-static approximation, i.e., it is assumed that the index varies on a time scale long compared with the transit time of a photon through the medium. Hence, terms proportional to the time derivative of the refractive index are neglected, but the parametric time dependence of the refractive index is retained.

For axial symmetry with respect to the z-axis, Eqs. (1) can be combined to give

$$\frac{\partial^2 \tilde{r}}{\partial z^2} = \frac{1}{\tilde{n}}\left(1+\left(\frac{\partial \tilde{r}}{\partial z}\right)^2\right)\left(\frac{\partial \tilde{n}}{\partial \tilde{r}} - \frac{\partial \tilde{r}}{\partial z}\frac{\partial \tilde{n}}{\partial z}\right), \tag{2}$$

where $\tilde{r}(z)$ is the radial position of a ray at axial location z.

ii) Ray Distribution

The propagation of a laser beam through a refractive medium can be described by a distribution of N rays in the phase space $(\mathbf{r},\mathbf{v})$, i.e.,

$$f(\mathbf{r},\mathbf{v},z) = \sum_{i=1}^{N} \delta(\mathbf{r}-\tilde{\mathbf{r}}(\mathbf{r}_{0i},\mathbf{v}_{0i},z))\delta(\mathbf{v}-\tilde{\mathbf{v}}(\mathbf{r}_{0i},\mathbf{v}_{0i},z)) \tag{3}$$

where $\mathbf{r}$ and $\mathbf{v}$ denote transverse ray position and transverse velocity, respectively. The quantities $\tilde{\mathbf{r}}(\mathbf{r}_{0i},\mathbf{v}_{0i},z)$ and $\tilde{\mathbf{v}}(\mathbf{r}_{0i},\mathbf{v}_{0i},z)$ are the phase space trajectories of the i^{th} ray with phase space coordinates $(\mathbf{r}_{0i},\mathbf{v}_{0i})$ at $z=0$. These trajectories evolve according to Eqs. (1) or (2). In the limit of a large number of rays, a continuous distribution can be formed, i.e.,

$$f(\mathbf{r},\mathbf{v},z) = \int d^2 r_0 \; d^2 \mathrm{v}_0 \; f(\mathbf{r}_0,\mathbf{v}_0,0)\; \delta(\mathbf{r}-\tilde{\mathbf{r}}(\mathbf{r}_0,\mathbf{v}_0,z))\delta(\mathbf{v}-\tilde{\mathbf{v}}(\mathbf{r}_0,\mathbf{v}_0,z)). \tag{4}$$

The number density of rays, $\int d^2\mathrm{v}\, f(\mathbf{r},\mathbf{v},z)$, is proportional to the intensity. For an axially symmetric laser beam, the intensity at position (r, z) is given by

$$I(r,z) = \int I(r_0,0) g(\mathbf{v}_0) \frac{\delta(r - \tilde{r}(r_0,\mathbf{v}_0,z))}{r} r_0 dr_0 d^2\mathrm{v}_0, \tag{5}$$

where the subscript zero denotes an initial ($z = 0$) value, and $g(\mathbf{v}_0)$ is the initial transverse velocity distribution normalized so that $\int g(\mathbf{v}_0) d^2\mathrm{v}_0 = 1$.

iii) Optical Beam Quality

The laser spot size is defined as $R(z) \equiv \left\langle \tilde{r}^2(r_0,\mathbf{v}_0,z) \right\rangle^{1/2}$, where the averaging operator for any quantity Q is $\langle Q \rangle = (4\pi/P) \int Q(r_0,\mathbf{v}_0,z) I(r_0,0) g(\mathbf{v}_0) r_0 dr_0 d^2\mathrm{v}_0$,

and P is the beam power. It can be shown that the spot size satisfies $R''(z) = \varepsilon^2 / R^3(z)$, where

$$\varepsilon^2 \equiv \left\langle \tilde{r}^2 \right\rangle \left\langle (\tilde{r}')^2 + \tilde{r}\tilde{r}'' \right\rangle - \left\langle \tilde{r}\tilde{r}' \right\rangle^2 \tag{6}$$

and $\partial\varepsilon^2/\partial z = \left\langle \tilde{r}^2 \right\rangle \left\langle 3\tilde{r}'\tilde{r}'' + \tilde{r}\tilde{r}''' \right\rangle$. The quantity ε is the optical equivalent of particle beam emittance [5]. In a uniform medium, $\tilde{r}'' = 0$ and ε^2 is a constant of motion ($\partial\varepsilon^2/\partial z = 0$). The optical beam quality parameter is defined as

$$M^2 = \pi\varepsilon/\lambda \tag{7}$$

and is proportional to the rms area of the ray distribution in optical phase space. For a fundamental Gaussian beam, $\varepsilon = \lambda/\pi$ and $M^2 = 1$.

In a uniform medium, the equation for the spot size has the solution

$$R^2(z) = R_0^2 \left(1 - \frac{z}{L_f} \right)^2 + \theta^2 z^2, \tag{8}$$

where L_f is a constant that determines the focal length and the asymptotic spreading (diffraction) angle is given by $\theta = \varepsilon / R_0 = M^2 \theta_0$, where $\theta_0 = \lambda/(\pi R_0)$ is the diffraction angle of a Gaussian beam. Hence, M^2 is the ratio of the spreading angle of a beam to the diffraction angle of a Gaussian beam with an equivalent spot size. The asymptotic spreading angle of the optical beam is referred to as M^2 "times diffraction-limited."

iv) Diffraction

The ray equations are valid in the limit where $\lambda \to 0$ and hence, do not describe diffraction. However, diffraction can be introduced in an ad hoc fashion by giving the rays a transverse velocity distribution that results in the intensity profile remaining Gaussian and having the correct vacuum diffraction angle.

To obtain the correct velocity distribution, we evaluate ε for a Gaussian beam with an initial intensity profile $I(r, z=0) = (2P/\pi R_0^2)\exp(-2r^2/R_0^2)$. The velocity distribution of the rays is taken to have the form $g(\mathbf{v}_0) = (1/\pi \bar{\mathrm{v}}^2)\exp\left(-|\mathbf{v}_0|^2/\bar{\mathrm{v}}^2\right)$, where $\bar{\mathrm{v}}$ is the transverse velocity spread. A Gaussian velocity distribution ensures that the intensity profile remains Gaussian when propagating in vacuum. For a focused Gaussian beam propagating in vacuum, Eq. (2) can be integrated to obtain $\tilde{r}(z) = r_0 + \left[(\mathrm{v}_0/c) - (r_0/L_f)\right]z$. Using this result to evaluate ε in Eq. (6) and setting $M^2 = 1$ yields the velocity spread $\bar{\mathrm{v}} = \theta_0 c/\sqrt{2} = \lambda c/(\sqrt{2}\pi R_0)$, which gives a spreading angle equal to the Gaussian diffraction angle.

III. Effects of Nonlinearities on Optical Beam Quality

We derive a general expression for M^2 due to the lowest order (dominant) geometrical, thermal, or other nonlinear aberrations in a thin lens. The thin lens approximation states that the change

in the radial position of a ray as it passes through a lens is negligible. It is also assumed that (1) the beam is Gaussian, (2) thermal and other nonlinear effects are proportional to the beam intensity, and (3) the transverse extent of the nonlinear medium is much larger than the laser spot size. With these assumptions, the angle of a ray after it passes though a thin lens can be written as

$$\begin{aligned} \tilde{r}' &= \beta_0 + \frac{\partial}{\partial r}\left[L(r)(n(r)-1)\right]_{r=\tilde{r}} \\ &\approx \beta_0 + \alpha_1 \frac{\tilde{r}}{R_0} + \alpha_2 \left(\frac{\tilde{r}}{R_0}\right)^2 + \alpha_3 \left(\frac{\tilde{r}}{R_0}\right)^3 + O\left(\frac{\tilde{r}^4}{R_0^4}\right), \end{aligned} \tag{9}$$

where $\beta_0 = \mathrm{v}_0 / c$ is the angle of the ray before it enters the lens, $L(r)$ is the lens thickness and the constants α_j are functions of the geometrical and nonlinear aberrations. Using Eq. (9) to evaluate M^2 in Eq. (7), and noting that $\left\langle \tilde{r}^n \right\rangle = 2^{1-(n/2)}\Gamma(1+(n/2))R_0^n$, results in

$$M^2 = \left[1 + \frac{\pi^2 R_0^2}{\lambda^2}\left(\left(1 - \frac{9\pi}{32}\right)\alpha_2^2 + \frac{3}{8}\sqrt{\frac{\pi}{2}}\,\alpha_2\alpha_3 + \frac{1}{2}\alpha_3^2\right)\right]^{1/2}. \tag{10}$$

The quantities α_2 and α_3 contain terms describing the lowest order geometrical aberrations and other terms which are proportional to nonlinear refractive index of the lens. The nonlinear refractive index of a lens contains contributions from many physical processes, for example, thermal effects, electronic vibration (optical Kerr effect), and electrostriction, among others [6].

In the steady state, the effective nonlinear index due to thermal effects is approximately given by

$$n_{2,T} = \gamma(2R_L^2 / R_0^2)\left(\frac{\partial n}{\partial T}\right)\frac{\alpha R_0^2}{8\kappa},$$

where R_L is the lens radius, R_0 is the laser spot size, $\partial n/\partial T$ is the thermo-optic constant, α is the absorption coefficient, κ is the thermal conductivity of the lens, and $\gamma(x)$ is a function of order unity that is defined in Sec. IV. For a typical BK7 lens with $\partial n/\partial T = 10^{-5}\,K^{-1}$, $\alpha = 5\times10^{-4}\,\mathrm{cm}^{-1}$, $R_L = 2.5\,\mathrm{cm}$, and a laser beam with $R_0 \sim 1\,\mathrm{cm}$, the effective nonlinear index due to thermal effects is $n_{2T} \sim 3\times10^{-8}\,\mathrm{cm}^2/\mathrm{W}$, which is much larger than the electronic nonlinear index, i.e., the optical Kerr effect, for which $n_{2K} \sim 10^{-16}\,\mathrm{cm}^2/\mathrm{W}$. Hence, from here on, we retain only the dominant thermal nonlinearity.

IV. Thermal Nonlinearity in Lenses

A laser beam with spot size R_0 passing through a lens with radius $R_L > R_0$ will non-uniformly heat the lens and modify its optical properties. We calculate the steady state temperature profile and, in the following Section, calculate its effect on beam quality. We assume that the absorption coefficient of the lens is small enough that we can neglect attenuation of the laser within the lens. The temperature within the lens satisfies the heat equation,

$$\rho_0 C_p dT/dt = \kappa\nabla^2 T + \alpha I(r), \tag{11}$$

where ρ_0 is the lens mass density, C_p is the specific heat, κ is the thermal conductivity, α is the absorption coefficient, and $I(r)$ is the laser intensity. Within the lens, it is assumed that the heat flux in the longitudinal direction is much smaller than in the transverse direction, i.e., the temperature is uniform in the longitudinal direction. Hence, we neglect longitudinal derivatives in the heat equation and treat temperature as solely a function of radial coordinate and time. In solving Eq. (11), the boundary conditions are taken to be 1) the radial derivative of the

temperature is zero at $r = 0$, and 2) the edge of the lens is maintained at a specified temperature, $T(R_L) = T_\infty$, where R_L is the radius of the lens.

For a cw laser beam, the temperature profile will approach a steady state on a time scale $\tau_T \sim \rho_0 C_p R_0^2 / \kappa$, where R_0 is the spot size of the laser beam. Assuming a Gaussian laser intensity profile, i.e., $I(r) = I_0 \exp(-2r^2 / R_0^2)$, Eq. (11) has an analytic steady state solution given by

$$\begin{aligned} \Delta T(r) = T(r) - T_\infty &= \overline{T}\left[\Gamma\left(0, \frac{2R_L^2}{R_0^2}\right) - \Gamma\left(0, \frac{2r^2}{R_0^2}\right) - \ln\left(\frac{r^2}{R_L^2}\right)\right] \\ &= \Delta T(0) + \overline{T}\sum_{n=1}^{\infty} a_{T,2n}\left(\frac{r^2}{R_0^2}\right)^n, \end{aligned} \tag{12}$$

where $\overline{T} \equiv \alpha P/(4\pi\kappa)$, $a_{T,2n} = (-2)^n/(n\,n!)$, and $\Gamma(n,x)$ is the incomplete Gamma function. The steady-state temperature change on-axis is given by $\Delta T(0) = \gamma\left(2R_L^2/R_0^2\right)\overline{T}$, where $\gamma(x) = \gamma_0 + \Gamma(0,x) + \ln(x)$, and $\gamma_0 \approx 0.58$ is Euler's constant. Figure 2 plots the radial temperature profile [Eq. (12)] normalized to $\overline{T}$ for various values of R_L / R_0.

We consider the propagation of a high-power laser beam through a lens with a non-zero absorption coefficient and spherical surfaces as shown in Fig. 1 and calculate the beam quality modification due to thermal effects. It is assumed that the beam spot size is much smaller than the radius of curvature of the lens so that only the lowest order spherical aberration is retained.

To lowest order in the temperature change, ΔT, the angle of a ray at radial position r_0 after passing through a lens is given by

$$\tilde{r}_0' = \beta_0 + \frac{\partial}{\partial r}\left[L_C(r)\left((n_0 - 1) + g\Delta T(r)\right)\right]_{r=r_0}, \tag{13}$$

where $\beta_0 = v_0/c$ is the angle of the ray before it enters the lens, n_0 is the linear refractive index, $g = (\partial n/\partial T) + (n_0 - 1)\alpha_T$, α_T is the thermal expansion coefficient, and $L_C(r)$ is the lens thickness in the absence of thermal effects. In writing Eq. (13), we have made the thin-lens approximation, i.e., the radial position of a ray does not change as it passes though the lens.

For a spherical lens,

$$\begin{aligned} L_C(r) &= L_o + R_{C1}\left[1-\left(1-\frac{r^2}{R_{C1}^2}\right)^{1/2}\right] + R_{C2}\left[1-\left(1-\frac{r^2}{R_{C2}^2}\right)^{1/2}\right], \\ &\approx L_0\left[1 + a_{C,2}\left(\frac{r}{R_0}\right)^2 + a_{C,4}\left(\frac{r}{R_0}\right)^4 + O\left(\frac{r^6}{R_0^6}\right)\right] \end{aligned} \tag{14}$$

where R_{C1} and R_{C2} are the radii of curvature of the two faces as indicated in Fig. 1, $a_{C,2} = (R_0^2/2L_0)(R_{C1}^{-1} + R_{C2}^{-1})$ and $a_{C,4} = (R_0^4/8L_0)(R_{C1}^{-3} + R_{C2}^{-3})$, and L_0 is the lens thickness on axis. The second line of Eq. (14) is an expansion for $r << R_{C1}, R_{C2}$ which retains the lowest order spherical aberration.

In the analysis that follows we assume a Gaussian laser beam and a bi-convex or bi-concave lens for which $R_{C1} = R_{C2} = R_C$, and $R_C > 0$ ($R_C < 0$) denotes a bi-concave (bi-convex) lens. For a bi-convex lens, the lens radius, R_L, is limited by geometry, i.e.,

$$R_L < R_C\left[1-\left(1-\frac{L_0}{2R_C}\right)^2\right]^{1/2} \approx (L_0 \mid R_C \mid)^{1/2}.$$

In the vacuum region after the lens, $r_0'' = 0$, so that $\varepsilon^2 \equiv \langle \tilde{r}_0^2 \rangle \langle \tilde{r}_0'^2 \rangle - \langle \tilde{r}_0 \tilde{r}_0' \rangle^2$. Substituting Eqs. (12) and (14) into Eq. (13) gives

$$\tilde{r}_0' = \beta_0 + \alpha_1\left(\frac{r_0}{R_0}\right) + \alpha_3\left(\frac{r_0}{R_0}\right)^3 + O\left(\frac{r_0^5}{R_0^5}\right), \tag{15a}$$

$$\alpha_1 = [(n_0 - 1) + g\Delta T(0)]\frac{2R_0}{R_C} - \frac{4L_0}{R_0} g\bar{T}, \tag{15b}$$

$$\alpha_3 = [(n_0 - 1) + g\Delta T(0)]\left(\frac{R_0^3}{R_C^3}\right) + g\bar{T}\frac{4L_0}{R_0}\left(1 - \frac{2R_0^2}{R_C L_0}\right). \tag{15c}$$

Equation (10) then yields (for $\alpha_2 = 0$), $M^2 = [1 + \Delta_{SA} + \Delta_T]^{1/2}$ where

$$\Delta_{SA} = (n_0 - 1)^2 \frac{\pi^2 R_0^2}{2\lambda^2}\left(\frac{R_0^6}{R_C^6}\right), \tag{16a}$$

$$\Delta_T = 4g\bar{T}(n_0 - 1)\frac{\pi^2 R_0^2}{\lambda^2}\left(\frac{R_0^2 L_0}{R_C^3}\right)\left(1 - \frac{2R_0^2}{R_C L_0}\right) \tag{16b}$$

are lowest order modifications to the beam quality due to spherical aberration (Eq. (16a)), and lens heating (Eq. (16b)). In writing Eqs. (16), we have assumed that the temperature change is sufficiently small that we can neglect terms that are of order $(g\bar{T})^2$ and that $g\Delta T(0) << n_0 - 1$. Eqs. (16) are valid when $\Delta_{SA} >> |\Delta_T|$. When $2R_0^2/(L_0|R_C|) < 1$, Δ_T has the same sign as R_C, i.e., the temperature aberration increases M^2 when $R_C > 0$ (concave lens) and decreases M^2 when $R_C < 0$ (convex lens). When $2R_0^2/(L_0|R_C|) > 1$, the thermal aberration decreases M^2 independent of the sign of R_C.

A more accurate calculation requires that more terms be kept in the representation of temperature since the expansion parameter $r_0^2/R_0^2 > 1$ for rays near the edges of the intensity distribution. Additionally, one can relax the requirement that the laser spot size be much less the lens radius. In this case, it can be shown that

$$\Delta_{SA} = \delta^3 \frac{(n_0 - 1)^2}{\theta_0^2} h_1(f), \tag{17a}$$

and

$$\Delta_T = 8g\bar{T}\frac{(n_0-1)}{\theta_0^2}\left(\frac{\delta^2}{f\sigma}\right)\sum_{n=1}^{\infty}\frac{(-1)^{n+1}2^n}{(n+1)!}\left[1-\frac{(n+1)^2}{2n}f\sigma\right]h_n(f), \qquad (17b)$$

where $f = R_0^2/R_L^2$ is the lens filling factor, $\sigma = R_L^2/(R_C L_0)$, $\delta = R_0^2/R_C^2$, $h_n(f) = \gamma_2(f)\gamma_{2n+4}(f) - \gamma_4(f)\gamma_{2n+2}(f)$,

$$\gamma_n(f) = 2^{1-(n/2)}\left[\Gamma(1+(n/2)) - \Gamma\left(1+(n/2),\frac{2}{f}\right)\right],$$

$\Gamma(n)$ is the Gamma function, and $\Gamma(n,x)$ is the incomplete Gamma function. For a bi-convex lens, $|\sigma|<1$. The sum in Eq. (17b) requires $\sim O(R_L^2/R_0^2)$ terms to converge. The functions $h_n(f)$ are positive definite. Letting $f \to 0$ and retaining only the first term in Eq. (17b) recovers Eqs. (16).

When analyzing Eqs. (17) and in the numerical simulations that follow, we will consider lenses made of either BK7 glass or optical-grade fused silica. Laser absorption in fused silica in the infrared is primarily due to the OH^- content, which can vary by orders of magnitude depending on the type of fused silica and how it is manufactured. Suprasil W-1 is a variant of fused silica with an extremely low OH content of < 3ppm [7] and an absorption coefficient ~ 10^{-6} cm^{-1} at 1 μm [8]. Optical-grade fused quartz has an OH content of ~ 400-500 ppm and an absorption coefficient of ~ 10^{-5} cm^{-1}, while standard UV-grade fused silica has a higher OH content of > 1000 ppm [9]. The thermo-optical properties of these two materials, summarized in Table 1, are taken from Ref. [10] except for the absorption coefficients of BK7 and fused silica, which were measured in our laboratory. The fused silica lens used in these measurements had an OH content of > 1000 ppm. The value of $\partial n/\partial T$ for fused silica was estimated from Ref. [10].

Figure 3 plots Δ_{SA} and Δ_T (Eq. (17)) as functions of the normalized laser beam spot size, R_0/R_L, for a bi-concave ($R_C > 0$) and bi-convex ($R_C < 0$) lens. The lens is assumed to be BK7

glass with $n_0 = 1.45$, $|R_C| = 30$ cm, $R_L = 3$ cm, and $L_0 = 1$ cm. The laser wavelength is 1μm and the power is 1 kW. It is seen that the thermal aberration increases M^2 for $R_C > 0$ and decreases M^2 for $R_C < 0$.

V. Numerical Simulation

We have developed a ray optics code based on solving Eq. (2) for an axially symmetric distribution of rays which pass through an arbitrarily specified refractive index $n(r,z,t)$. The time dependence of n is due to heating and is self-consistently obtained by solving Eq. (11) using the boundary conditions discussed in Section IV. When calculating the temperature profile, a Gaussian intensity profile is assumed with a spot size given by $R(z) \equiv \left\langle \tilde{r}^2(r_0, \mathbf{v}_0, z) \right\rangle^{1/2}$. Diffraction is modeled by assuming a distribution of transverse velocities as specified in Section III. We assume a cw, Gaussian beam that turns on at $t = 0$ and calculate the beam quality after passing through a collection of lenses. Although the input beam is assumed to be Gaussian, the model places no limitations on M^2 as the beam propagates through the optical system. We first consider the case of single bi-convex or bi-concave lenses to compare with the analysis of the previous Section. We then model a beam director configuration that was used in a recent series of high-power fiber laser experiments performed by NRL in which thermal effects were observed [3].

i) Single Lens

We consider the case of a single bi-convex or bi-concave spherical lens with the same parameters used in plotting Fig. 3. The laser wavelength is 1 μm and the spot size is $R_0 = 1.25$ cm. The steady-state time constant for the temperature is $\tau_T \sim \rho_0 C_p R_0^2 / \kappa \sim 5$

minutes. Figure 4a plots the on-axis temperature change, $\Delta T(0)$, as a function of time. Figure 4b plots M^2 versus time for a bi-convex (blue curve) and a bi-concave (red curve) lens. At $t = 0$, in the absence of heating, $M^2 \approx 2.7$ for both the concave and convex lenses. Since the quantity $4|\sigma|f \sim 0.2$ is less than unity for these parameters, M^2 decreases (increases) as the temperature increases for the bi-convex (bi-concave) lens, consistent with the analysis of the previous Section. The beam quality reaches a steady state in ~ 5 minutes. In the steady-state, $M^2 \approx 3.2$ for the concave lens and $M^2 \approx 2.2$ for the convex lens.

Figure 5 plots M^2 in the steady state versus laser power for different lens thicknesses for convex and concave lenses. For the case of a bi-concave lens, $M^2 \sim 2.7$ when the power is near zero and increases with power and lens thickness. For a bi-convex lens, $M^2 \sim 2.7$ when the power is near zero and, for the two thinner lenses, decreases as the beam power is increased over the range plotted. For the thicker lens, M^2 initially decreases and then increases with power. A minimum M^2 of ~ 1.4 is obtained when the power is ~ 4 kW.

ii) NRL Beam Expander

The earlier beam expander configuration used in the NSWC experiment had five lenses made of various optical materials such as fused silica and BK7. In that experiment, it was observed that beam quality deteriorated severely when the laser power approached ~ 1 kW. This was attributed to thermal effects in the optics. A more recent version of the NRL beam expander is a 3-lens system made of uv-grade fused silica that we model here to examine the effects of thermal aberrations.

A schematic diagram of the beam expander is shown in Fig. 6 with the lens parameters and geometry listed in Table 1. The first two plano-concave lenses expand the beam from a spot

size of 1.25 cm to 2.5 cm. The short focal lengths of these first two lenses introduce a large degree of spherical aberration which is corrected by the third lens. For an input beam with $M^2 = 1$, in the absence of thermal aberrations, the beam quality is $M^2 \sim 4$ after the first lens, $M^2 \sim 20$ after the second lens, and $M^2 \sim 1$ after the third collimating lens. This low-power limit has been successfully benchmarked against the ZEMAX optical design code [11].

In the presence of thermal aberrations, M^2 increases with laser power. Figure 7 plots the output M^2 versus laser power for a beam expander made from BK7 lenses (dashed curve) and fused silica lenses (solid curve). The thermo-optical properties of each material are listed in Table 1. For simplicity, it is assumed that the refractive indices of both materials are $n = 1.45$. Compared with fused silica, BK7 has higher absorption and thermal expansion coefficients, but a lower thermo-optic coefficient. The overall result is that M^2 increases faster with increasing laser power for the BK7 configuration, e.g., for a laser power of ~ 1.5 kW, $M^2 \sim 3$ for the BK7 lenses and $M^2 \sim 1.2$ for fused silica lenses.

In Figure 8, we start with a beam expander with three fused silica lenses, replace one of the lenses with BK7, and plot M^2 versus laser power. It is seen that the beam quality has a stronger dependence on laser power (M^2 increases faster with laser power) when it is the first lens that is replaced with BK7. The weakest dependence results from replacing the third lens. Comparing with Fig. 7, we note that when the first lens is BK7 and the second and third lenses are fused silica, the resulting M^2 is larger than that of case where all the lenses are BK7. Also, the beam expander in which lenses 1 and 2 are fused silica and lens 3 is BK7 has a *lower* M^2 than a beam expander in which all of the lenses are made of fused silica.

VI. Discussion

We calculate the laser propagation efficiency for the conditions of the NRL experiment at SOR and compare with the observations. The propagation efficiency is defined as the ratio of the power on a target to the transmitted power. For a single Gaussian beam with power P_0 and a target of radius R_{target} at range L, the propagation efficiency is given by $\eta = P_{\text{target}} / P_0 = \exp(-\beta L)\left[1 - \exp(-2R_{\text{target}}^2 / R^2(L))\right]$, where P_{target} is the power on the target and [3]

$$R(L) = R(0)\left(\frac{\lambda L}{\pi R^2(0)}\right)\left(M^4 + \frac{2R^2(0)}{\rho_o^2}\right)^{1/2} \tag{18}$$

is the beam spot size on the target, $R(0)$ is the spot size after exiting the beam expander, $\rho_o = 0.158\left(\lambda^2 / (C_n^2 L)\right)^{3/5}$ is the transverse coherence length due to turbulence, and C_n^2 is the turbulence strength parameter [2]. In writing Eq. (18), it is assumed that the focal length is equal to the range to the target and that $M^2 \sim 1$. Equation (18) becomes less accurate when $M^2 >> 1$ because of the coupling of higher order modes with turbulence.

The propagation efficiency is plotted in Fig. 9 as a function of laser power for the conditions of the experiment, i.e., $\lambda = 1\mu\text{m}$, $C_n^2 = 10^{-15}\,\text{m}^{-2/3}$, $L = 3\text{km}$, $\beta = 0.08\,\text{km}^{-1}$, and $R_{\text{target}} = 10$ cm. It is seen that for BK7 lenses, the propagation efficiency decreases rapidly with laser power when $P_0 > 500\,W$. For fused silica, the propagation efficiency remains relatively constant (~ 80%) for laser powers < 2 kW. Hence, a kW-class beam director using transmissive optics will require the use of a low-absorption material such as fused silica.

The value of M^2 from the laser is measured in the laboratory to be 1.1 ± 0.05 at 1 kW of power. It is observed that M^2 increases by 30% after passing through the beam expander using

all fused silica lenses. Theoretically, from Fig. 7, M^2 increases by ~20% at 1 kW. There are several differences between the beam expander modeled here, and the actual beam expander used in the experiments that may account for this difference. First, we have neglected the heating and convection of the air between the lenses. The beam expander lenses, when used in the experiment, were sealed inside a metal mounting tube which could enhance the heating of the air surrounding the lenses. Second, lens misalignment due to heating of the lens mounts is not accounted for in the model. Third, the theoretical radial boundary condition on the temperature profile may not be accurate for laser spot sizes comparable to the lens radius. Using a boundary condition that assumes radiative loss at the edge of the lens results in a larger temperature change. However, in this parameter regime, the beam quality is not affected significantly by the choice of boundary conditions. Fourth, there is uncertainty in our experimental measurements of the absorption coefficient of the lenses. Lastly, we note that significant beam degradation occurs within the laser source itself when it is run at higher power (~ 2 kW).

VII. Conclusions

We have analyzed and modeled the propagation of a high-power laser beam through a lens and calculated the optical beam quality resulting from geometrical aberrations and thermal nonlinearities. It is found that for a thin, spherical lens in the low-power regime, thermal aberrations can either enhance or degrade the beam quality depending on the value of the parameter $\sigma \equiv 2R_0^2/(L_0|R_C|)$ and the curvature of the lens (convex or concave) . When $\sigma < 1$, the temperature aberration increases M^2 for concave lens and decreases M^2 for a convex lens. When $\sigma > 1$, the thermal aberration decreases M^2 independent of the sign of R_C .

We have modeled a 3-lens optical beam expander similar to that used in recent high-power fiber laser experiments performed by NRL. It is found that when using kilowatt-class lasers and transmissive optics, low-absorption material such as optical-grade fused silica is required to achieve high propagation efficiencies over kilometer ranges.

Acknowledgments

This work is supported by the Office of Naval Research and the High Energy Laser Joint Technology Office.

References

1. "2kW CW Yb-Doped Fiber Laser with Record Diffraction Limited Brightness," V. Gapontsev, CLEO Europe, CJ1-1-THU, Munich, Germany, 2005.
2. "Laser Beam Propagation through Random Media," L.C. Andrews, R.L. Phillips, 2nd Ed., SPIE Press, Bellingham, WA , 2005.
3. "Incoherent Combining and Atmospheric Propagation of High-Power Fiber Lasers For Directed-Energy Applications," P. Sprangle, A. Ting, J. Peñano, R. Fischer, and B. Hafizi, to appear in IEEE, J. Quant. Elec. (Jan. 2009); Laser Focus World vol. **44**, Issue 8, Aug. 2008, Web article http://www.laserfocusworld.com/articles/331428.
4. "The Classical Theory of Fields," L.D. Landau and E.M. Lifshitz, 4th ed., Pergamon Press, Oxford (1975).
5. "Theory and Design of Charged Particle Beams," M. Reiser, Wiley & Sons, New York (1994).
6. "Nonlinear Optics," R. Boyd, 2nd ed., Academic Press, San Diego, CA (2003).
7. "Properties and structure of vitreous silica. I ," R. Bruckner, J. Non-Crystalline Solids **5**, 123 (1970)
8. "Calorimetric study of optical absorption of Suprasil W-1 fused quart at visible, near-IR, and near-UV wavelengths," R.T. Swimm, Y. Xiao, M. Bass, App. Opt. **24**, 322 (1985)
9. Del Mar Photonics, http://www.sciner.com/Opticsland/FS.htm
10. W.J. Tropf, M.E. Thomas, and T.J. Harris in Handbook of Optics vol 2, 2nd ed, McGraw-Hill, New York, NY (1995).
11. ZEMAX Development Corporation, http://www.zemax.com

Material	BK7	Fused Silica
α: Absorption coefficient	3×10^{-4} cm^{-1}	5×10^{-5} cm^{-1}
κ: Thermal conductivity	1.1×10^{-2} W/(cm K)	1.4×10^{-2} W/(cm K)
$\partial n/\partial T$	2.3×10^{-6} K^{-1}	10^{-5} K^{-1}
$\alpha_T = L^{-1}\partial L/\partial T$	7.1×10^{-6} K^{-1}	5.1×10^{-7} K^{-1}
ρ_0: density	2.5 g/cm^3	2.2 g/cm^3
C_p: heat capacity	0.86 J/(g K)	0.75 J/(g K)

Table 1: Thermal and optical parameters for BK7 and uv-grade fused silica used in the models. Parameters are taken from Ref. [10], except for the absorption coefficients of BK7 and fused silica, which were measured in the lab. The value of $\partial n/\partial T$ for fused silica was estimated from Ref. [10].

	Lens 1	**Lens 2**	**Lens 3**
Position, z_i	0	1.5856 cm	17.59 cm
Thickness, L_i	0.62 cm	0.62 cm	2 cm
Curvature	$R_{C1} = 18.03$ cm	$R_{C2} = 15.45$ cm	$R_{C31} = -64.607$ cm $R_{C32} = -20.7975$ cm

Table 2: Lens geometry parameters for the 3-lens NRL beam expander. Position, z_i, denotes the z-coordinate of the left face of the lens. L_i denotes the on-axis thickness. For lens 3, R_{C31} (R_{C32}) is the radius of curvature of the left (right) face. The radial dependence of the lens thickness in the absence of thermal effects has the form of Eq. (14).

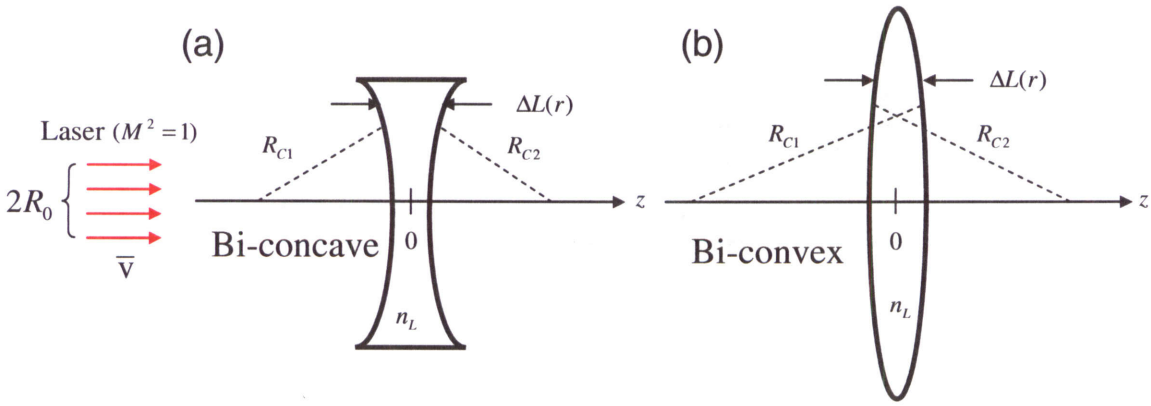

Figure 1: Schematic diagram of (a) bi-concave and (b) bi-convex spherical lenses with linear refractive index $n_L(r,z)$ and radii of curvature R_{C1} and R_{C2} The quantity $\Delta L(r)$ denotes the lens thickness at radial position r. A laser beam (ray distribution) with an initial spot size R_0, transverse velocity spread $\overline{v}$, and $M^2 = 1$ propagates along the z axis.

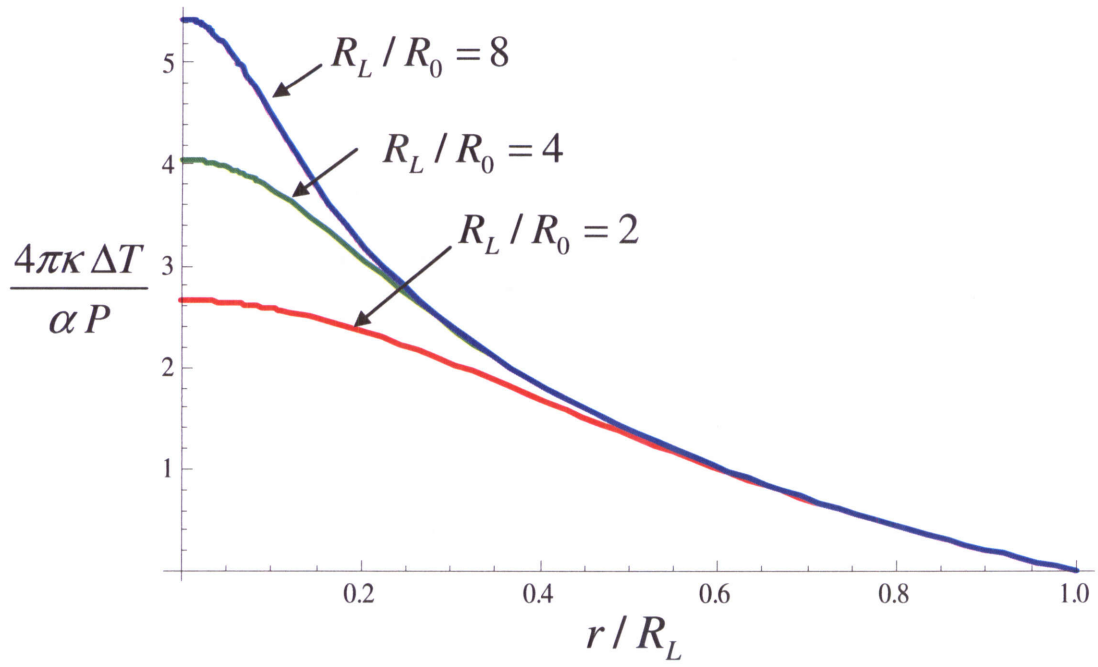

Figure 2: Normalized steady state temperature change [Eq. (10)] versus normalized radial coordinate for $R_L / R_0 = 2$ (red), 4 (green), and 8 (blue), where R_L is the lens radius, R_0 is the laser spot size, and $\Delta T = T(r) - T_\infty$.

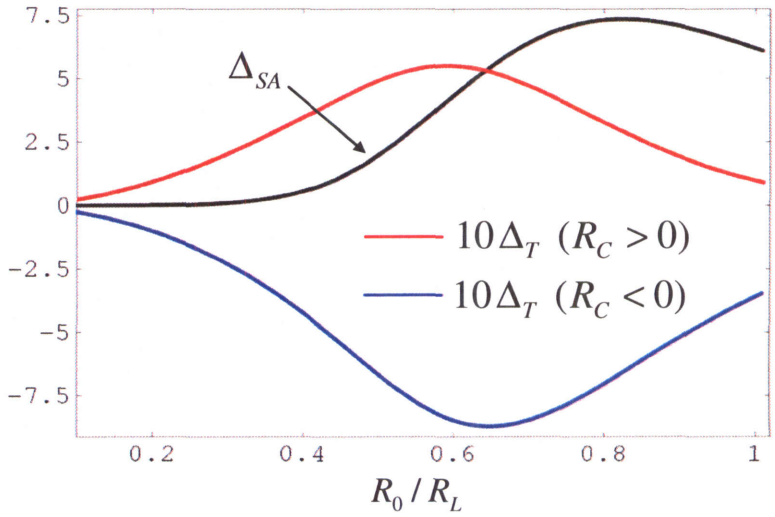

Figure 3: Beam quality modification due to spherical aberration (Δ_{SA}) and thermal aberration (Δ_T) versus laser beam spot size. The laser spot size, R_0, is normalized to the lens radius, R_L. The beam quality is given by $M^2 = [1 + \Delta_{SA} + \Delta_T]^{1/2}$. Curves denote Δ_{SA} (black curve, Eq. (13)) and $10\Delta_T$ (Eq. (14)) for a bi-concave (red curve) and a bi-convex (blue curve) lens. A BK7 lens is assumed with $n_0 = 1.45$, $|R_C| = 30$ cm, $R_L = 3$ cm, $L_0 = 1$ cm. The laser wavelength is 1μm and the power is 1 kW.

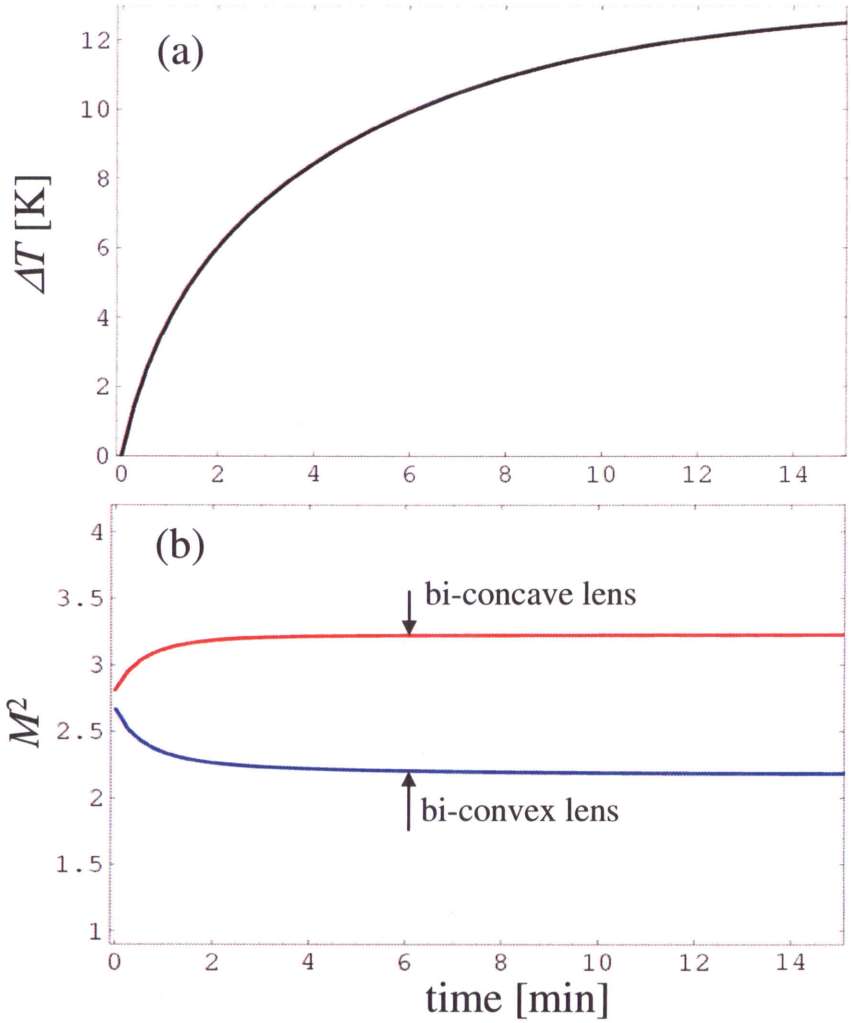

Figure 4: Peak temperature (Fig. a) and beam quality (Fig. b) versus time for a bi-concave (red curve) and bi-convex (blue curve) lens. The lens parameters are the same as in Fig. 3. The laser wavelength is $1\mu m$, $R_0 = 1.25$ cm, and the power is 2 kW.

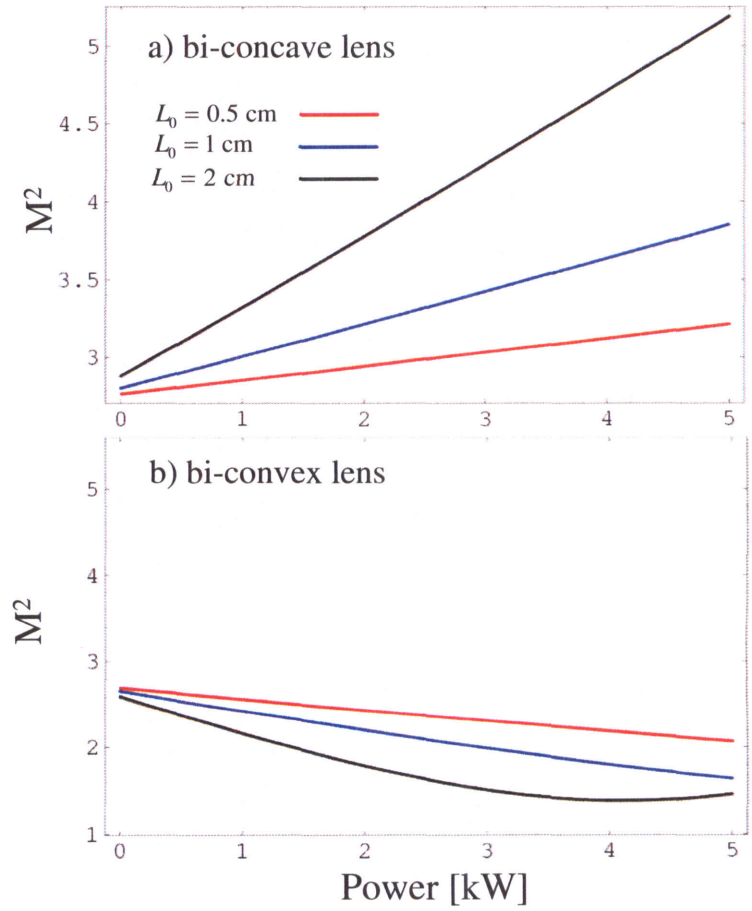

Figure 5: Steady state beam quality, M^2, versus laser beam power for a single (a) bi-concave and (b) bi-convex BK7 lens with thickness $L_0 = 0.5$ cm (red curves), $L_0 = 1$ cm (blue curves), and $L_0 = 2$ cm (black curves). The other lens parameters are the same as in Fig. 3.

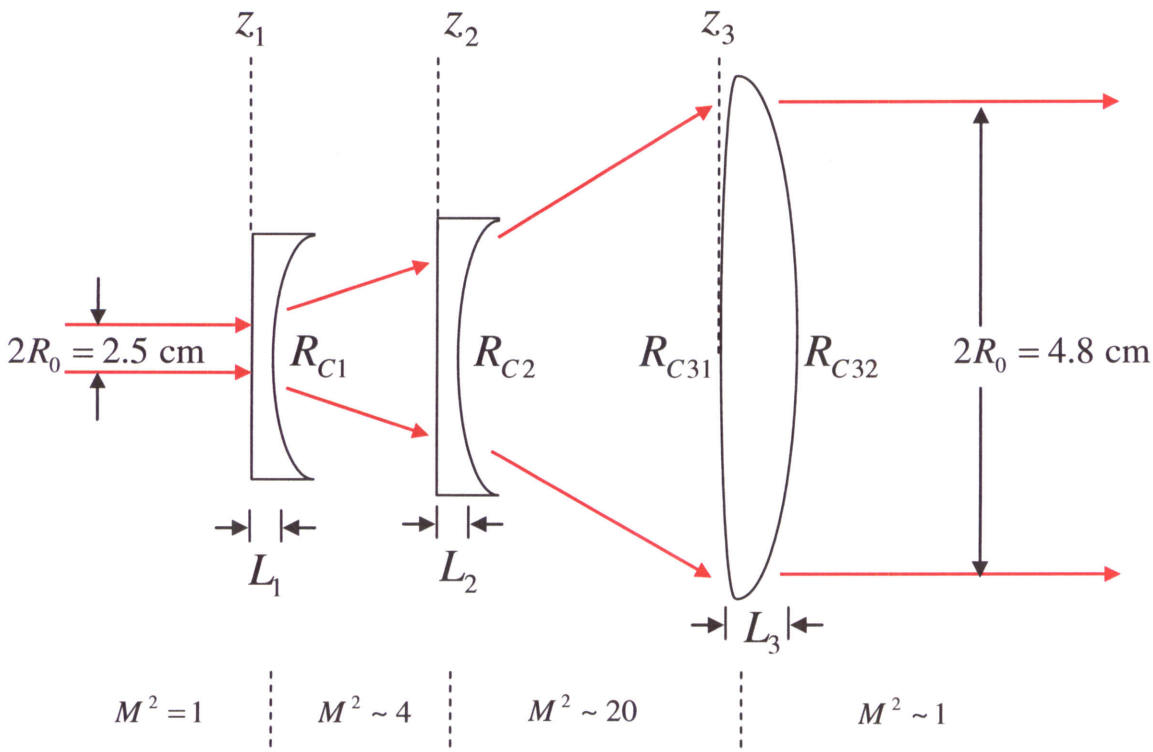

Figure 6: Schematic diagram of the NRL high-power fiber laser beam expander. Lens geometry is listed in Table 2. A kW-class beam of diameter ~ 2.5 cm is expanded to a diameter of ~ 4.8 for propagation in the atmosphere. Lens parameters are listed in Table 1. For an input beam wit $M^2 \sim 1$, the beam quality is $M^2 \sim 4$ after the first lens, $M^2 \sim 20$ after the second lens, and $M^2 \sim 1$ after the third lens, in the absence of thermal effects.

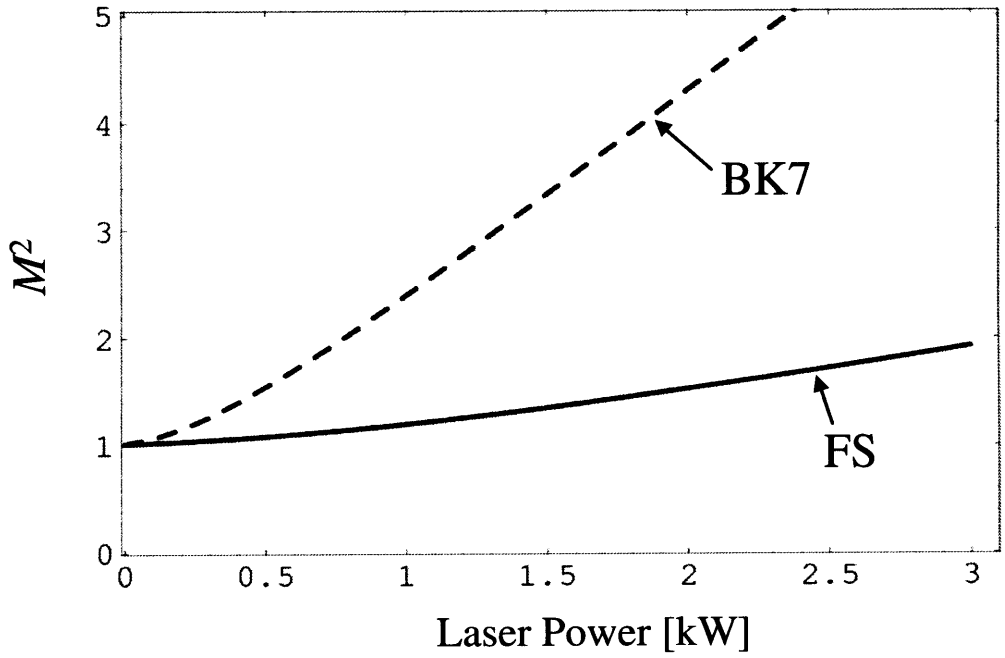

Figure 7: (a) Steady state beam quality versus laser power at the output of the expander shown in Fig. 6. Fused silica (FS) and BK7 lenses are assumed with parameters given in Table 1.

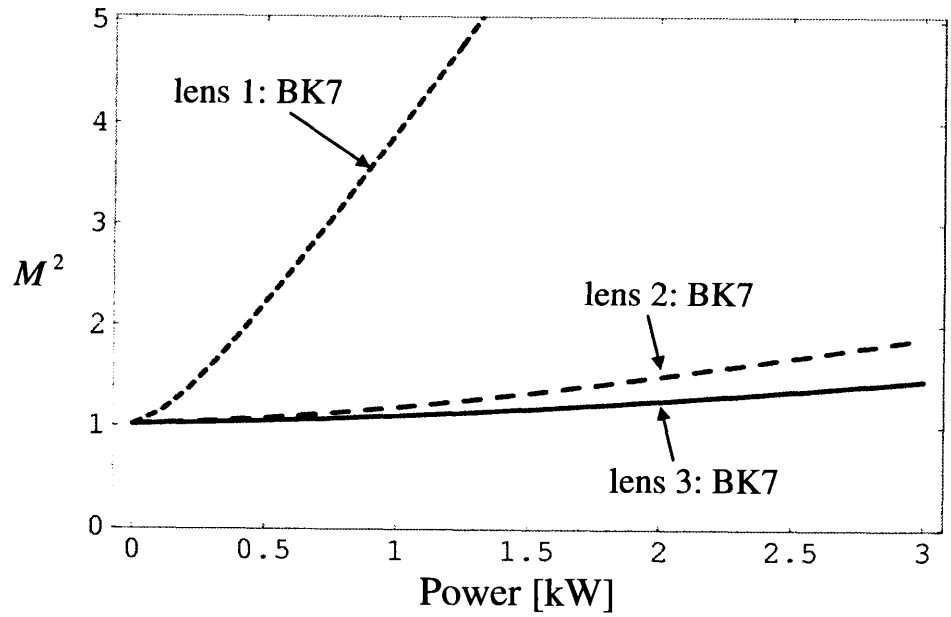

Figure 8: Steady-state M^2 versus power for the NRL beam expander with one BK7 lens and two fused silica lenses. Lens parameters are listed in Table 1. Curves denote cases where lens 1 (short dashes), 2 (longer dashes), or 3 (solid curve) is BK7. The laser wavelength is 1 μm, and the initial spot size $R_0 = 1.25$ cm.

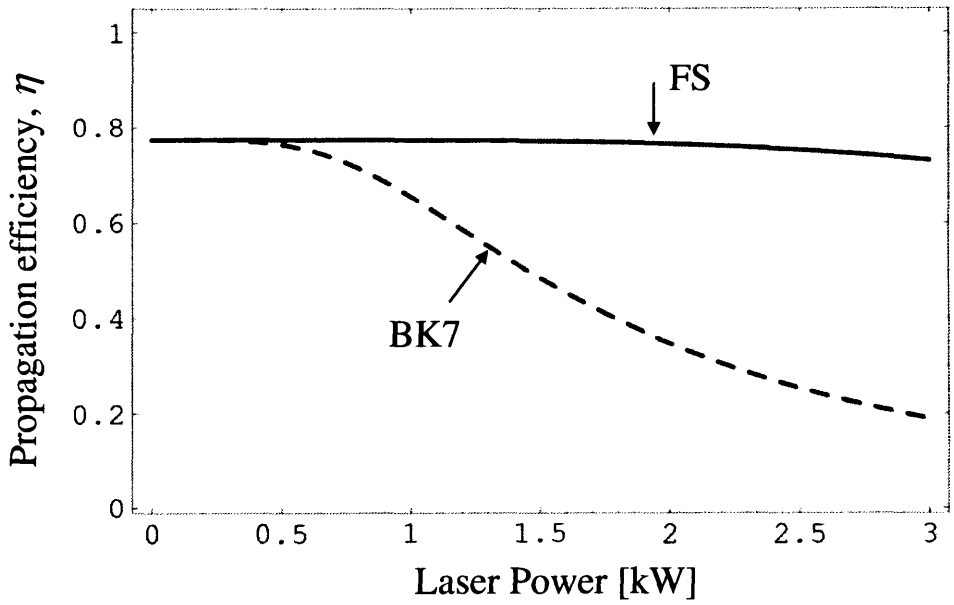

Figure 9: Propagation efficiency versus laser power for the beam expander configuration of Fig. 6 with BK7 lenses (dashed curve) and fused silica lenses (solid curves). Propagation parameters are typical of the NRL SOR experiments, i.e., $\lambda = 1\mu\text{m}$, $C_n^2 = 10^{-15}\,\text{m}^{-2/3}$, $L = 3.2\,\text{km}$, $\beta = 0.08\,\text{km}^{-1}$, and target radius, $R_{\text{target}} = 10\,\text{cm}$.